

A New Structure of Buck-Boost Z-Source Converter Based on Z-H Converter

E. Babaei*, T. Ahmadzadeh

Faculty of Electrical and Computer Engineering, University of Tabriz, Tabriz, Iran.

Abstract- In this paper, a new structure for buck-boost Z-source converter based on Z-H topology is proposed. The proposed converter consists of two LC networks similar to the conventional Z-source and Z-H converters. One of the characteristics of the proposed structure is that, without any changing in its' power circuit, it can be used in different conversions such as dc/dc, dc/ac and ac/ac. This unique characteristic of the proposed structure is similar to matrix converters. To use this structure in different conversions just control system should be changed. Other main advantages of the proposed converter are simpler topology, step-up and step-down capabilities and low ripple in voltage and current waveforms. Due to capabilities of the proposed converter mentioned above, it can be used in applications such as connect renewable energy sources to the grid, speed control of induction machines, electric vehicles and etc. In this paper, a complete analysis of the proposed converter in dc/dc conversion with details and mathematical equations is presented. Moreover, for the proposed topology, the ripple of inductors and capacitors is given. A suitable control method is presented, too. Also, the power losses and efficiency of the proposed converter are calculated. The correctness operation of the proposed converter is reconfirmed by the experimental results.

Keyword: Buck-boost dc/dc converter, LC network, Shoot-through (ST) state, Z-H converter, Z-source inverter.

1. INTRODUCTION

The conventional voltage source converters are extensively used in industry. Nevertheless, they have their own conceptual and theoretical limitations. The voltage source inverters are step-down for dc/ac conversion and step-up for ac/dc conversion. To obtain a desired ac output voltage, in conditions which overdrive requires and the available dc voltage is limited, an additional dc/dc boost converter is necessary. It is noticeable that the additional power converter decreases efficiency and increases system cost. The upper and lower devices of each phase leg cannot be gated on simultaneously because of occurring a shoot-through and destructing the devices. Besides, the conventional current source converters have their own conceptual and theoretical limitations. The current source inverters are step-up for dc/ac conversion and step-down for ac/dc conversion. In current source converters, at least one of the upper and lower devices has to be gated on. If not, an open circuit of the dc inductor occurs and destroys the devices.

In Ref. [1], a Z-source converter has been presented to overcome the problems of the conventional voltage source and current source converters. Also, the control method of Z-source converter for dc/ac, ac/dc, ac/ac and dc/dc conversions has been provided. The main circuit of Z-source converter connects by two impedance source networks (LC networks) in X shape to the dc source, load or another converter. In the conventional voltage source and current source converters, a capacitor and inductor are used, respectively. Hence, the unique features in Z-source converter do not exist in them. The Z-source concept can be applied to all dc/ac [2], ac/dc [3], ac/ac [4], and dc/dc [5] conversions.

Up to now, several modified PWM control techniques for a Z-source inverter have been presented in order to gain simple implementation, low device stress and less commutation per switching cycle. The SPWM and SVPWM modulation techniques for 2-level three-phase H-bridge topologies are extensively used. In addition, other methods of modulation will be described as follows:

Some of sinusoidal PWM (SPWM) modulation techniques are simple boost control [1, 6], maximum boost control and maximum boost control with third-harmonic injection [6, 7], constant boost control and constant boost control with third-harmonic injection [8, 9]. In [10], some of SPWM modulation techniques have been compared in terms of the voltage gain. In simple boost control method, shoot-through states created for

Received: 15 May 2015

Revised: 15 Nov. 2015 and 5 Apr. 2016

Accepted: 12 Aug. 2016

*Corresponding author:

E-mail: e-babaei@tabrizu.ac.ir (E. Babaei)

step-up voltage. To create shoot-through states, a carrier triangular signal is compared to the three phase sinusoidal reference signal and two straight lines. Disadvantage of this modulation technique is that when the shoot-through range increases, the modulation index decreases. Also, for the application which needs a higher voltage boost, the device rating is increased. In [6], for solving this issue, maximum boost control and maximum boost control with third-harmonic injection methods have been presented. Maximum boost control method in comparison with simple boost control method increases the boost factor range. Nevertheless, the shoot-through time intervals are variable in this method. Hence, low-frequency ripple generates in the capacitor voltage and inductor current. This issue causes increasing size and cost of the LC network components. To solve these problems, the maximum constant boost control and constant boost control with third-harmonic injection methods have been proposed [7, 8]. In these control methods, the maximum boost factor achieves and the time intervals of shoot-through states are constant which eliminates the low-frequency harmonic component in the LC network. Another efficient modulation technique for conventional inverter topologies is space vector pulse width modulation (SVPWM) control method. In this control method, the commutation time of switches and the harmonic of the output voltage/current are efficaciously reduced. Also, the voltage stress and switching loss decreased because of the suitable dc-link voltage. These unique characteristics in SVPWM control method can be applied for various Z-source converters. It should be noted that, for keeping the advantages of SVPWM control method in the Z-source converters, the shoot-through switching state should correctly inserted in the switching cycle without any change in the volt-sec balance.

In [11-14], some of the SVPWM techniques have been presented for Z-source topologies. By creating two new modifications in SVPWM control method, experiments and performance analysis have been presented [15, 16]. In addition, modified SVPWM techniques have been given to reduce the common mode voltage and currents for photovoltaic systems [17, 18] and motor drives [19].

In [20], a switched-inductor Z-source inverter topology using two batteries has been presented. This inverter is capable of increasing the output voltage level in comparison to the other structures of Z-source inverter in lower duty cycle. As a result, the presented topology is more effective in improvement of the output power quality. In [21], a structure for quasi-Z-source

inverters based on the combination of switched inductors and transformers has been presented. In the presented inverter, the high voltage gain is achieved by increasing the ratio of the transformer and the number of switched inductor cells that can reduce efficiency. In [22], to reach high voltage gain with high efficiency, a new topology for boost Z-source inverter based on switched-inductor cell has been presented. Having common earth between the input source and inverter and capability to generate higher voltage gain by using lower amount of the duty cycles are some advantages of the presented Z-source inverter. In [23], a topology for half-bridge switched boost Z-source inverter has been presented. The presented half-bridge inverter uses more active elements rather than capacitors and inductors in comparison with the conventional half-bridge Z-source inverter that results in reduction of weight, size and cost. Moreover, the presented inverter has the capability of eliminating inverter leg short circuit issues and is able to further increase the output voltage level in comparison with its conventional types.

In Z-source converters, a diode or a switch is essential preceding of the LC network. This diode (or switch) creates discontinuity in the current. This issue creates an unwanted operation mode in during the non-shoot-through switching state. Moreover, this diode (or switch) prevents the reverse current. Hence, these converters are applied only when there is no need for energy return to input source [24, 25]. In [25], a Z-H converter has been presented by using the concept of Z-source converter. In the structure of Z-H converter also used a LC network but it is different in terms of connection. So that, the LC network of the Z-H converter has two ports in its' input and four ports in its' output. Two input ports of the LC network are connected to two ports of the input source, and its' four output ports are connected to one H-bridge. Two ports and two middle points of the H-bridge are connected to two capacitors and two inductors respectively. In addition, the Z-H converter compared to the Z-source inverter eliminates diode preceding of LC network and shoot-through switching state. The Z-H topology directly can be applied to dc/dc, dc/ac, ac/dc and ac/ac conversions without any change in its structure similar to the Z-source topology [25-27].

In this paper, a new buck-boost Z-source converter based on Z-H topology is proposed. One of the advantages of the proposed converter is the positive and negative output voltage. It is noticeable that this feature can be used in electrochemical power supply. In electrochemical power supply, sometimes it requires positive voltage and other times it needs negative

voltages. Moreover, the magnitude of the positive and negative voltages is different. One of the other characteristics of the proposed structure is that, without any changing in its' power circuit, the proposed structure can be used in different conversions such as dc/dc, dc/ac and ac/ac. This unique characteristic of the proposed structure is similar to matrix converters. To use this structure in different conversions, just the control system should be changed. The difference of the proposed structure with matrix converters is that in matrix converters due to not using of energy storage elements, the converter does not have ability to be operated in step-up mode. Whereas the proposed structure due to the use of energy storage elements can be used in both step-up and step-down modes. Because the proposed topology can act as dc/dc, dc/ac and ac/ac operations, so the proposed converter can be replaced with some dc/dc, dc/ac and ac/ac converters based on Z-source converters. Due to capabilities of the proposed converter, it can be used in applications such as connect renewable energy sources to the grid, speed control of induction machines, fuel cell systems, photovoltaic systems, wind turbines, motor drives, electric vehicles and etc. Also, the Z-source concept can be easily applied to adjustable-speed drive (ASD) systems. The Z-source rectifier/inverter system can produce an output voltage greater than the ac input voltage by controlling the boost factor, which is impossible for the conventional ASD systems. Moreover, the proposed converter in ac/ac conversion theoretically, can boost the ac voltage to any desired magnitude. A very big difference compared to the Z-source ac/ac converter is that the output voltage of the proposed ac/ac converter is a sinusoidal waveform. Therefore, the main advantages of proposed converter in ac/ac conversion are simple structure and not needing any additional filter in circuit.

Also, the details of calculation of voltages and currents of all components are presented in this paper. Moreover, for the proposed topology, the ripple of inductors and capacitors is given. A suitable control method is presented, too. In addition, the power losses and efficiency of the proposed converter are calculated. Since there is no need to any changes in power circuit of converter for different conversions, so in this paper, only the operation and analysis of the proposed converter in dc/dc conversion with details and mathematical equations is presented. It is noticeable that, the operation and analysis of the proposed converter at other conversions are same with dc/dc conversion. The experimental results are given to validate the correctness operation of the proposed converter.

2. PROPOSED BUCK-BOOST Z-SOURCE CONVERTER

Fig. 1 shows the power circuit of the proposed buck-boost Z-source converter. The proposed converter consists of four bidirectional switches and two LC networks. It is distinct in terms of connection with conventional Z-source and Z-H converters.

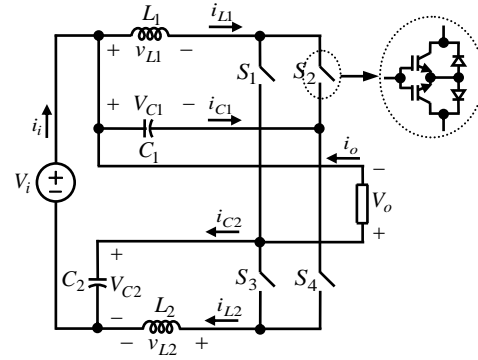


Fig. 1. The proposed buck-boost Z-source converter.

Considering Fig. 1, the switches S_1 and S_2 are complementary controlled. There is same condition for S_3 and S_4 . When the switches S_1 and S_4 are turned on, the switches S_2 and S_3 are turned off simultaneously, and when the switches S_2 and S_3 are turned on, the switches S_1 and S_4 are turned off. The duty cycle for the switches S_2 and S_3 is considered D . The proposed converter has two $D=[0, 0.5)$ and $D=(0.5, 1]$ operating zones. In the first operating zone, the converter operates in buck-boost operation, and in the second operating zone, the converter is only in boost operation. Fig. 2 shows the control signals for both operating zones of $D=[0, 0.5)$ and $D=(0.5, 1]$. The equivalent circuits of converter in T_0 (which the switches S_2 and S_3 are turned on) and T_1 (which the switches S_1 and S_4 are turned on) time intervals for both operating zones are shown in Fig. 3.

Assuming same values for L_1 and L_2 inductors ($L_1 = L_2 = L$) and also same values for C_1 and C_2 capacitors ($C_1 = C_2 = C$), the following results are achieved:

$$V_{C1} = V_{C2} = V_C \tag{1}$$

$$v_{L1} = v_{L2} = v_L \tag{2}$$

Where, V_C and v_L are the voltages across the capacitors and inductors, respectively.

For T_0 time interval (Fig. 3(a)), the following equations can be written:

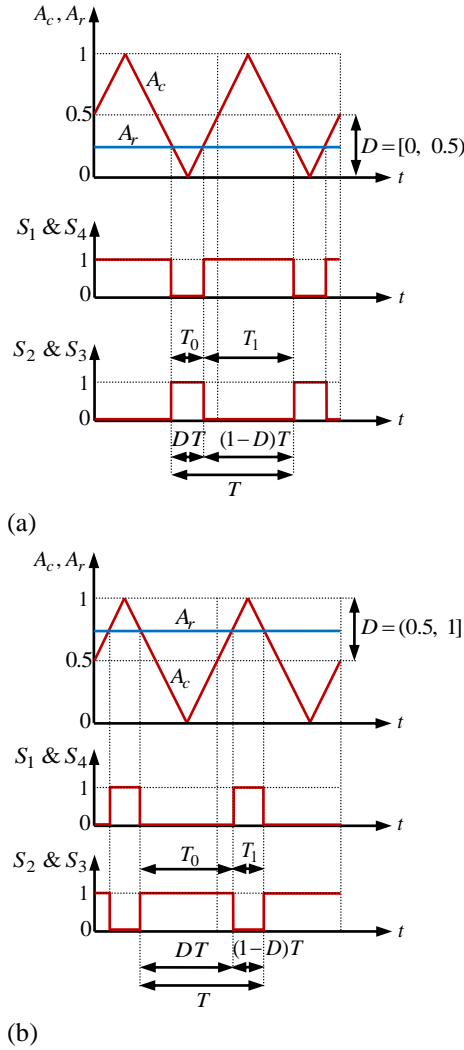


Fig. 2. The control signals, (a) in $D=[0, 0.5]$ operating zone, (b) in $D=(0.5, 1]$ operating zone.

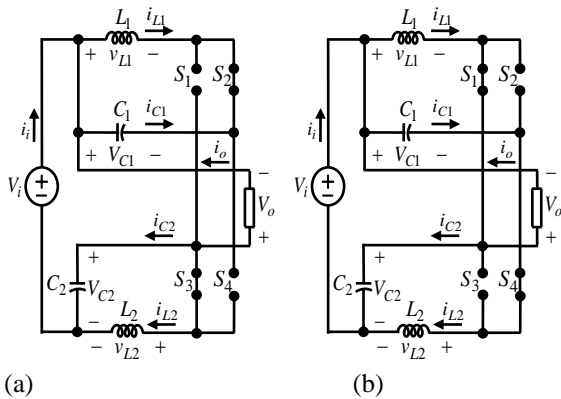


Fig. 3. The equivalent circuits, (a) in T_0 time interval, (b) in T_1 time interval.

$$v_{L,T0} = V_C \quad (3)$$

$$V_{o,T0} = V_C - V_i \quad (4)$$

Where, V_i and V_o are the input and output voltages of converter, respectively.

For T_1 time interval (Fig. 3(b)), the following equations are obtained:

$$v_{L,T1} = V_i - V_C \quad (5)$$

$$V_{o,T1} = V_C - V_i \quad (6)$$

According to Eqs. (4) and (6), the value of output voltage is equal in both time intervals of T_0 and T_1 .

Considering the voltage balancing law, the average voltage of an inductor is zero. So, from Eqs. (3) and (5), the voltages across the capacitors can be obtained as follows:

$$V_C = \frac{T_1}{T_1 - T_0} V_i = \frac{1-D}{1-2D} V_i > 0 \text{ for } D = [0, 0.5) \quad (7)$$

$$V_C = \frac{T_1}{T_1 - T_0} V_i = \frac{1-D}{1-2D} V_i < 0 \text{ for } D = (0.5, 1] \quad (8)$$

Where, $D = T_0/T$ is duty cycle of S_2 and S_3 switches.

By placing the value of V_C from Eqs. (7) and (8) into Eqs. (4) and (6), the output voltage in both operating zones and for all times is given by:

$$V_o = \frac{D}{1-2D} V_i > 0 \text{ for } D = [0, 0.5) \quad (9)$$

$$V_o = \frac{D}{1-2D} V_i < 0 \text{ for } D = (0.5, 1] \quad (10)$$

From Eqs. (9) and (10), the buck-boost factor (B) of converter can be defined as follows:

$$B = \frac{V_o}{V_i} = \frac{D}{1-2D} \text{ for } D = [0, 0.5) \& D = (0.5, 1] \quad (11)$$

In the first operating zone, B can be variable in ranges of $0 \leq B \leq 1$ (buck operation) and $1 \leq B \leq +\infty$ (boost operation). In the second operating zone, it can be variable in range of $-\infty < B \leq -1$ (only boost mode).

Fig. 4 shows the curves of voltage gain and stress voltage on capacitors versus duty cycle. Fig. 4 contains $D = [0, 0.5)$ and $D = (0.5, 1]$ operating zones. The value of output voltage is positive in the first operating zone and is negative in the second operating zone. In $D = [0, 0.5)$ operating zone, the proposed converter acts as buck-boost (buck in $0 \leq D \leq \frac{1}{3}$ and boost in

$\frac{1}{3} \leq D < 0.5$). In operating zone of $D = (0.5, 1]$, the converter is only in boost operation.

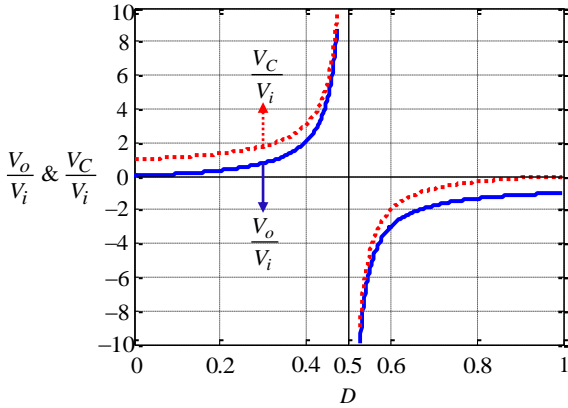


Fig. 4. Variations of the voltage gain and stress voltage on capacitors in terms of duty cycle.

In time interval of T_0 (Fig. 3(a)), the following equations are obtained:

$$i_{C1,T0} = i_{i,T0} + i_{o,T0} - i_{L1,T0} \quad (12)$$

$$i_{C2,T0} = i_{i,T0} - i_{L2,T0} \quad (13)$$

$$i_{C2,T0} = -i_{L2,T0} - i_{o,T0} \quad (14)$$

Where, i_c and i_l are the instantaneous currents through the capacitors and inductors, respectively. Also, i_i and i_o are the input and output currents of converter, respectively.

In time interval of T_1 (Fig. 3(b)), the following equations are obtained:

$$i_{C1,T1} = i_{i,T1} + i_{o,T1} - i_{L1,T1} \quad (15)$$

$$i_{C2,T1} = i_{i,T1} - i_{L2,T1} \quad (16)$$

$$i_{C1,T1} = i_{L2,T1} \quad (17)$$

$$i_{C2,T1} = i_{L1,T1} - i_{o,T1} \quad (18)$$

Assuming that the load is purely resistance (R_L), in both operating zones and for all times, the output current (i_o) and its' average value ($I_{o,av}$) is equal to:

$$i_o = I_{o,av} = \frac{V_o}{R_L} \quad (19)$$

From Eq. (3) and assuming that the initial currents of L_1 and L_2 inductors at the beginning of T_0 time interval are equal to $I_{1,L1}$ and $I_{1,L2}$, respectively, so, the currents through the inductors (i_{L1} and i_{L2}) in T_0 time interval are given by:

$$i_{L1,T0} = \frac{V_C}{L_1}t + I_{1,L1} \quad \text{for } 0 \leq t \leq T_0 \quad (20)$$

$$i_{L2,T0} = \frac{V_C}{L_2}t + I_{1,L2} \quad \text{for } 0 \leq t \leq T_0 \quad (21)$$

During T_0 time interval, the current through the inductors in the first operating zone is increased and in the second operating zone is decreased.

From Eq. (5) and assuming the new time origin, the initial currents of L_1 and L_2 inductors at the beginning of T_1 time interval are equal to $I_{2,L1}$ and $I_{2,L2}$, respectively, so, the currents through the inductors are given by:

$$i_{L1,T1} = \frac{V_i - V_C}{L_1}t + I_{2,L1} \quad \text{for } 0 \leq t \leq T_1 \quad (22)$$

$$i_{L2,T1} = \frac{V_i - V_C}{L_2}t + I_{2,L2} \quad \text{for } 0 \leq t \leq T_1 \quad (23)$$

During T_1 time interval, the current through the inductors in the first operating zone is decreased and in the second operating zone is increased.

Considering Eqs. (20) to (23), in order to transfer power from the input voltage source to output, in the first operating zone the voltage across the capacitors should be positive and their values are smaller than the input voltage source. Also, in the second operating zone the voltage across the capacitors should be negative and their values are greater than the input voltage source.

Assuming that there is no power losses in the converter, so, the following equation can be written:

$$V_i I_i = V_o I_o \quad (24)$$

By substituting the value of V_o from Eqs. (11) into (24), the average current of input voltage source ($I_{i,av}$) is equal to:

$$I_{i,av} = B I_{o,av} \quad (25)$$

3. CURRENT AND VOLTAGE RIPPLE CALCULATION

It should be noted that the currents through the inductors of L_1 and L_2 at the end of T_0 and T_1 time intervals are different, but both inductors have the same current ripple. So, in both operating zones, and considering Eqs. (7), (8) and (20) to (23), the current ripple of inductors can be achieved as follows:

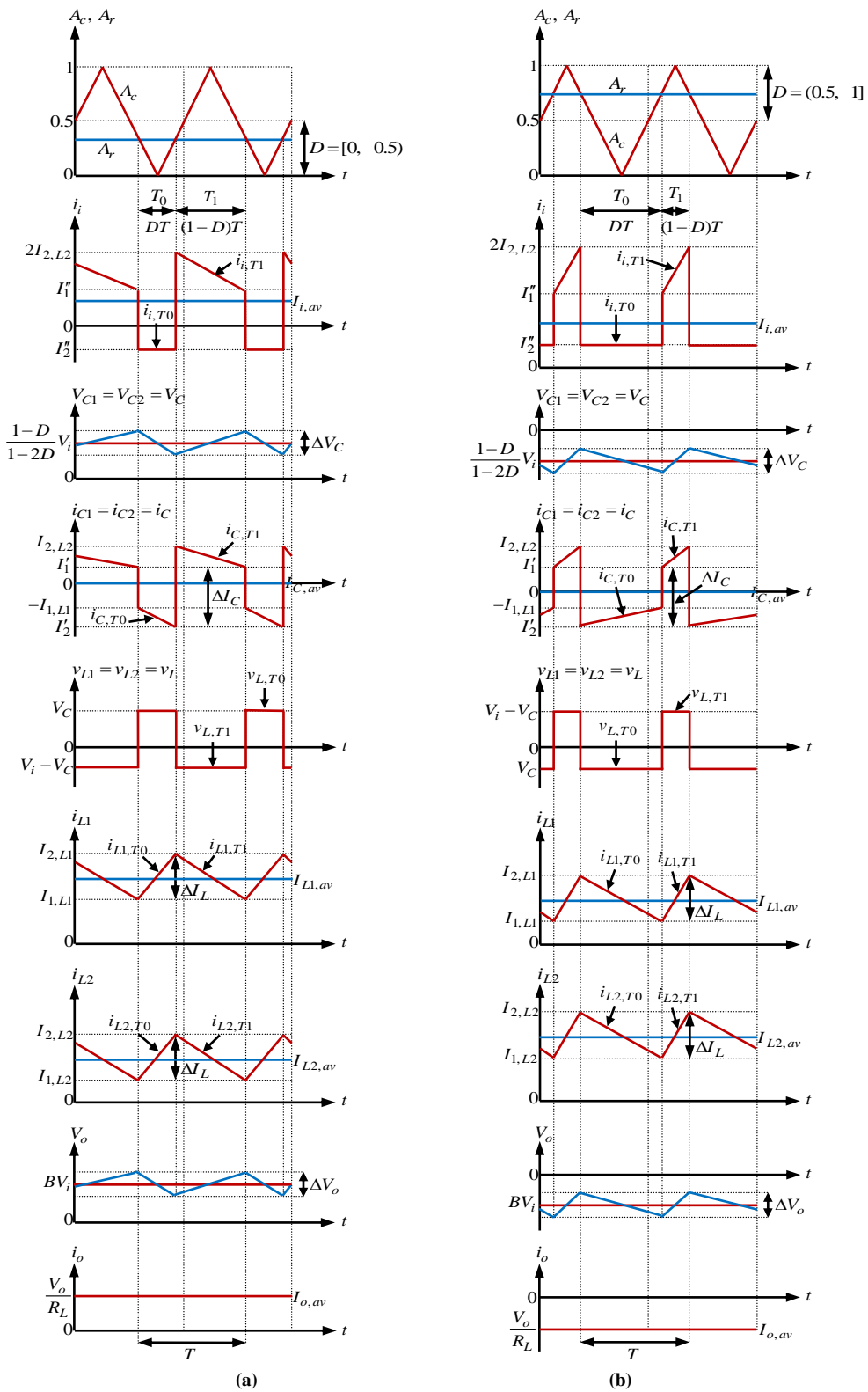


Fig. 5. Waveforms of the proposed converter, (a) operating zone of $D \in [0, 0.5]$, (b) operating zone of $D \in (0.5, 1]$.

$$\begin{aligned}\Delta I_{L1} = \Delta I_{L2} = \Delta I_L &= |I_{2,L1} - I_{1,L1}| = |I_{2,L2} - I_{1,L2}| \\ &= \frac{V_C}{L} DT = \left| \frac{D(1-D)}{1-2D} \right| \frac{V_i}{Lf}\end{aligned}\quad (26)$$

Where, $f = 1/T$ is the switching frequency of converter.

In steady state and according to the current balancing law, the average current of C_1 capacitor is zero. So, from Eqs. (12) and (15) and considering Eqs. (11), (19) and (25), the average current of L_1 inductor ($I_{L1,av}$) in both operating zones is given by:

$$I_{L1,av} = (1+B)I_{o,av} = \frac{D(1-D)}{R_L(1-2D)^2} V_i \quad (27)$$

Considering the current balancing law for C_2 capacitor, Eqs. (11), (13), (16), (19) and (25), the average current of L_2 inductor ($I_{L2,av}$) in both operating zones is equal to:

$$I_{L2,av} = BI_{o,av} = \frac{D^2}{R_L(1-2D)^2} V_i \quad (28)$$

The average current of inductors can also be calculated from the following equation:

$$I_{L1,av} = \frac{I_{1,L1} + I_{2,L1}}{2} \quad (29)$$

$$I_{L2,av} = \frac{I_{1,L2} + I_{2,L2}}{2} \quad (30)$$

Also, the current ripple of inductors can be obtained as follows:

$$\Delta I_L = I_{2,L1} - I_{1,L1} = I_{2,L2} - I_{1,L2} \quad (31)$$

From Eqs. (29) to (31), in both operating zones, the currents through the inductors at the end of T_0 and T_1 time intervals are given by:

$$I_{2,L1} = \frac{2I_{L1,av} + \Delta I_L}{2} \quad (32)$$

$$I_{1,L1} = \frac{2I_{L1,av} - \Delta I_L}{2} \quad (33)$$

$$I_{2,L2} = \frac{2I_{L2,av} + \Delta I_L}{2} \quad (34)$$

$$I_{1,L2} = \frac{2I_{L2,av} - \Delta I_L}{2} \quad (35)$$

Considering Eqs. (12) to (14), the capacitors current at the end of T_0 time interval (I'_2) is equal to:

$$I'_{2,C1} = I'_{2,C2} = I'_2 = -I_{2,L1} \quad (36)$$

Considering Eqs. (15) to (18), the capacitors current at the end of T_1 time interval (I'_1) is given by:

$$I'_{1,C1} = I'_{1,C2} = I'_1 = I_{1,L2} \quad (37)$$

From Eqs. (36) and (37), the current ripple of capacitors (ΔI_C) in both operating zones can be obtained as follows:

$$\Delta I_{C1} = \Delta I_{C2} = \Delta I_C = |I'_2 - I'_1| = |-I_{2,L1} - I_{1,L2}| \quad (38)$$

Considering Eq. (36), the voltage ripple across the capacitors (ΔV_C) in both operating zones can be achieved as follows:

$$\Delta V_{C1} = \Delta V_{C2} = \Delta V_C = \left| \pm \frac{D(I_{L1,av})}{Cf} \right| \quad (39)$$

By substituting Eq. (13) into Eq. (14), the current through the input voltage source at the end of T_0 time interval (I''_2) is given by:

$$i_{i,T0} \Big|_{t=T_0=DT} = I''_2 = -i_o \quad (40)$$

From Eqs. (16) and (37), the current through the input voltage source at the end of T_1 time interval (I''_1) is equal to:

$$i_{i,T1} \Big|_{t=T_1=(1-D)T} = I''_1 = 2I_{1,L2} \quad (41)$$

Considering Eqs. (1) to (41), the voltage and current waveforms of the proposed converter in both operating zones of $D = [0, 0.5)$ and $D = (0.5, 1]$ are shown in Fig. 5. It is noticeable that the proposed converter has step-down and step-up capability for dc/dc and ac/ac conversions, whereas for dc/ac conversion has only step-up capability. In Table 1, the final equations for different conversions have been summarized. In Table 1, D_1 and D_2 are the duty cycle for $D_1 = [0, 0.5)$ and $D_2 = (0.5, 1]$ operating zones, respectively, and B_1 and B_2 are the boost factors for first and second operating zones. Also, V_m and f_i are the amplitude and frequency of input voltage source, respectively.

Table 1. The final equations for different conversions of the proposed converter.

Power conversion	Output voltage	The voltage across the capacitors	The voltage across the inductors		Capability
			$v_{L,T0}$	$v_{L,T1}$	
dc/dc	BV_i	$\frac{1-D}{1-2D}V_i$	$\frac{1-D}{1-2D}V_i$	$-\frac{D}{1-2D}V_i$	step-down and step-up
dc/ac	$\frac{1}{1-2D_1}V_i = B_1V_i > 0$	$\frac{1-D_1}{1-2D_1}V_i$	$\frac{1-D_1}{1-2D_1}V_i$	$-\frac{D_1}{1-2D_1}V_i$	Only step-up
	$\frac{1}{1-2D_2}V_i = B_2V_i < 0$	$\frac{1-D_2}{1-2D_2}V_i$	$\frac{1-D_2}{1-2D_2}V_i$	$-\frac{D_2}{1-2D_2}V_i$	
ac/ac	$B(V_m \sin 2\pi f_i t)$	$\frac{1-D}{1-2D}[V_m \sin 2\pi f_i t]$	$\frac{1-D}{1-2D}[V_m \sin 2\pi f_i t]$	$-BV_m \sin 2\pi f_i t$	step-down and step-up

It is noticeable that the proposed converter has step-down and step-up capability for dc/dc and ac/ac conversions, whereas for dc/ac conversion has only step-up capability. In Table 1, the final equations for different conversions have been summarized.

4. DESIGN THE VALUES OF L AND C

Ripples of capacitor voltage and inductor current effect on stability of inverters. To properly design the values of C_1 and C_2 capacitors, the allowable voltage ripple $x_c\%$ may be used, which is defined as follows [27]:

$$x_{C1}\% = x_{C2}\% = x_C\% = \frac{\Delta V_C}{V_C} \quad (42)$$

Considering (27) and by substituting the values of V_C and ΔV_C from (7) and (39) into (42), the rated value of C_1 and C_2 capacitances is calculated as follows:

$$C_1 = C_2 = C = \frac{D(1-2D)(I_{L1,av})}{f(1-D)(V_i)x_C\%} = \frac{D^2}{fR_L(1-2D)x_C\%} \quad (43)$$

To properly design the values of L_1 and L_2 inductors, the allowable current ripples $x_{L1}\%$ and $x_{L2}\%$ are carried out, which is defined as follows: $x_{L1}\% = \frac{\Delta I_{L1}}{I_{L1,av}}$

$$x_{L2}\% = \frac{\Delta I_{L2}}{I_{L2,av}} \quad (44)$$

By substituting the values of ΔI_{L1} and $I_{L1,av}$ from Eqs. (26) and (27) into Eq. (44), and by placing the the values of ΔI_{L2} and $I_{L2,av}$ from Eqs. (26) and (28) into Eq. (45), the rated values of L_1 and L_2 inductances are calculated as follows:

$$L_1 = \frac{R_L(1-2D)}{f x_{L1}\%} \quad (46)$$

$$L_2 = \frac{R_L(1-D)(1-2D)}{Df x_{L2}\%} \quad (47)$$

5. CALCULATION OF POWER LOSSES AND EFFICIENCY

Assuming that each power electronic switch has a resistor R_T (indicating the forward resistance) and a voltage source V_T (indicating the forward voltage drop) which are series with switch, so, to calculate the power losses of one switch the following equation can be used:

$$P_S = P_{C,S} + P_{SW,S} \quad (48)$$

Where, $P_{C,S}$ and $P_{SW,S}$ are the conduction and switching power losses of S switch, respectively.

The conduction power losses of a switch can be obtained as follows [28]:

$$P_{C,S} = P_{R,S} + P_{VT} = (R_S I_{S,rms}^2) + (V_T I_{S,av}) \quad (49)$$

Where, $P_{R,S}$ and P_{VT} are the ohmic loss of S switch and the power loss associated with the forward voltage drop (V_T), respectively. Also, $I_{S,rms}$ and $I_{S,av}$ are the RMS and average currents through the S switch, respectively.

The switching power loss of a switch is equal to the sum of all turn on power loss ($P_{on,S}$) and turn off power loss ($P_{off,S}$) in a cycle of the output voltage. This can be written as follows:

$$P_{SW,S} = P_{on,S} + P_{off,S} = (E_{on,S} + E_{off,S})f \quad (50)$$

Where, $E_{on,S}$ and $E_{off,S}$ are the energy losses during the turn-on and turn-off time intervals of S switch, respectively.

To calculate the turn-on and turn-off energy losses of

a switch, we have:

$$E_{on,S} = \int_0^{t_{on,S}} v_S(t) i_S(t) dt \quad (51)$$

$$E_{off,S} = \int_0^{t_{off,S}} v_S(t) i_S(t) dt \quad (52)$$

Where, $v_S(t)$ and $i_S(t)$ are the instantaneous voltage and current of S switch, respectively.

Considering Figs. 1 and 3, the currents through the S_2 switch in time intervals of T_0 and T_1 can be calculated as follows:

$$i_{S2} = I_{L1,av} \quad \text{for } 0 \leq t \leq T_0 \quad (53)$$

$$i_{S2} = 0 \quad \text{for } 0 \leq t \leq T_1 \quad (54)$$

From Eqs. (53) and (54), the RMS current through the S_2 switch is equal to:

$$I_{S2,rms} = I_{L1,av} \sqrt{D} \quad (55)$$

Considering Eqs. (53) and (54), the average current through the S_2 switch is given by:

$$I_{S2,av} = \frac{1}{T} \int_0^T i_{S2} dt = I_{L1,av} \frac{T_0}{T} = DI_{L1,av} \quad (56)$$

By substituting the values of $I_{S2,rms}$ and $I_{S2,av}$ from Eqs. (55) and (56) into Eq. (49), we have:

$$P_{C,S} = (R_S I_{S,rms}^2) + (V_T I_{S,av}) \\ = DI_{L1,av} (R_{S2} I_{L1,av} + V_T) \quad (57)$$

It is noticeable that to calculate the turn-on and turn-off energy losses of a switch, the linear approximation of the voltage and current during switching period can be used [29], so, the energy losses during the turn-on time interval of S_2 switch is equal to:

$$E_{on,S2} = \int_0^{t_{on,S2}} v_{S2}(t) i_{S2}(t) dt = \frac{t_{on,S2}}{6} I_{L1,av} (V_C - v_L) \quad (58)$$

The energy loss during the turn-off time interval of S_2 switch is given by:

$$E_{off,S2} = \int_0^{t_{off,S2}} v_{S2}(t) i_{S2}(t) dt = \frac{t_{off,S2}}{6} I_{L1,av} (V_C - v_L) \quad (59)$$

By placing the values of $E_{on,S2}$ and $E_{off,S2}$ from Eqs. (58) and (59) into Eq. (50), we have:

$$P_{SW,S} = (E_{on,S} + E_{off,S}) f \\ = \frac{(V_C - v_L) I_{L1,av} f}{6} (t_{on,S2} + t_{off,S2}) \quad (60)$$

By substituting the values of $P_{C,S}$ and $P_{SW,S}$ from Eqs. (57) and (60) into Eq. (48), the power loss of S_2 switch is equal to:

$$P_{S2} = P_{C,S2} + P_{SW,S2} \\ = DI_{L1,av} (R_{S2} I_{L1,av} + V_T) \\ + \frac{(V_C - v_L) I_{L1,av} f}{6} (t_{on,S2} + t_{off,S2}) \quad (61)$$

According to Figs. 1 and 3, the currents through S_1 , S_3 and S_4 switches in time intervals of T_0 and T_1 can be calculated as follows:

$$i_{S1} = \begin{cases} 0 & \text{for } 0 \leq t \leq T_0 \\ I_{L1,av} & \text{for } 0 \leq t \leq T_1 \end{cases} \quad (62)$$

$$i_{S3} = \begin{cases} I_{L2,av} & \text{for } 0 \leq t \leq T_0 \\ 0 & \text{for } 0 \leq t \leq T_1 \end{cases} \quad (63)$$

$$i_{S4} = \begin{cases} 0 & \text{for } 0 \leq t \leq T_0 \\ I_{L2,av} & \text{for } 0 \leq t \leq T_1 \end{cases} \quad (64)$$

Considering Eqs. (48) to (64), the power losses of S_1 , S_3 and S_4 switches can be similarly calculated as follows:

$$P_{S1} = P_{C,S1} + P_{SW,S1} \\ = (1-D) I_{L1,av} (R_{S1} I_{L1,av} + V_T) \\ + \frac{(V_C - v_L) I_{L1,av} f}{6} (t_{on,S1} + t_{off,S1}) \quad (65)$$

$$P_{S3} = P_{C,S3} + P_{SW,S3} \\ = DI_{L2,av} (R_{S3} I_{L2,av} + V_T) \\ + \frac{(V_C - v_L) I_{L2,av} f}{6} (t_{on,S3} + t_{off,S3}) \quad (66)$$

$$P_{S4} = P_{C,S4} + P_{SW,S4} \\ = (1-D) I_{L2,av} (R_{S4} I_{L2,av} + V_T) \\ + \frac{(V_C - v_L) I_{L2,av} f}{6} (t_{on,S4} + t_{off,S4}) \quad (67)$$

Assuming that each capacitor has an equivalent series resistor (r_C), so, to calculate the ohmic loss of one capacitor the following equation can be used:

$$P_{rC} = r_C I_{C,rms}^2 \quad (68)$$

Where, $I_{C,rms}$ is the RMS current through the capacitor.

From Eqs. (12) and (17), the RMS current of C_1 capacitor can be obtained as follows:

$$I_{C1,rms} = \sqrt{\frac{1}{T} \int_0^T i_{C1}^2 dt} = \sqrt{D(I_{i,av} + I_{o,av} - I_{L1,av})^2 + (1-D)(I_{L2,av})^2} \quad (69)$$

By substituting the value of $I_{C1,rms}$ from Eq. (69) into Eq. (68), the ohmic power loss of C_1 capacitor is given by:

$$P_{rC1} = r_{C1} I_{C1,rms}^2 = r_{C1} D(I_{i,av} + I_{o,av} - I_{L1,av})^2 + r_{C1} (1-D)(I_{L2,av})^2 \quad (70)$$

From Eqs. (13) and (16), the RMS current of C_2 capacitor can be calculated as follows:

$$I_{C2,rms} = \sqrt{\frac{1}{T} \int_0^T i_{C2}^2 dt} = \sqrt{(I_{i,av} - I_{L2,av})^2 [D + (1-D)]} = I_{i,av} - I_{L2,av} \quad (71)$$

By placing the value of $I_{C2,rms}$ from Eq. (71) into Eq. (68), the ohmic power loss of C_2 capacitor is equal to:

$$P_{rC2} = r_{C2} I_{C2,rms}^2 = r_{C2} (I_{i,av} - I_{L2,av})^2 \quad (72)$$

Assuming that each inductor has a equivalent series resistor (r_L), so, to calculate the winding power loss of one inductor the following equation can be used:

$$P_{rL} = r_L I_{L,rms}^2 \quad (73)$$

Where, $I_{L,rms}$ is the RMS current through the inductor.

From Eq. (73), the winding power loss of L_1 and L_2 inductors can be calculated as follows:

$$P_{rL1} = r_{L1} I_{L1,rms}^2 = r_{L1} I_{L1,av}^2 \quad (74)$$

$$P_{rL2} = r_{L2} I_{L2,rms}^2 = r_{L1} I_{L2,av}^2 \quad (75)$$

The total power losses of the proposed buck-boost converter in dc/dc conversion can be expressed as:

$$P_{Loss} = (P_{S1} + P_{S2} + P_{S3} + P_{S4}) + (P_{rC1} + P_{rC2}) + (P_{rL1} + P_{rL2}) \quad (76)$$

Considering Eq. (76), the efficiency of the proposed converter can be obtained using the following equation:

$$\eta = \frac{P_o}{P_o + P_{Loss}} \quad (77)$$

6. CONSIDERING EQUIVALENT SERIES RESISTANCE (ESR)

In order to study the converter with presence of ESR capacitor, a resistor in series with the capacitor (R_C) should be considered.

Table 2. Comparison of the values obtained in states with and without ESR capacitors.

Parameters	Without ESR	With ESR	
$v_{L,T0}$	V_C	$V_C + V_{RC}$	
$v_{L,T1}$	$V_i - V_C$	$V_i - (V_C + V_{RC})$	
V_C	$\frac{1-D}{1-2D} V_i$	$\frac{1-D}{1-2D} V_i - V_{RC}$	
V_o	$\frac{D}{1-2D} V_i$	$\frac{D}{1-2D} V_i$	
i_o	$\frac{V_o}{R_L}$	$\frac{V_o}{R_L}$	
$i_{L,T0}$	$i_{L1,T0}$	$\frac{V_C}{L_1} t + I_{1,L1}$	$\frac{V_C + V_{RC}}{L_1} t + I_{1,L1}$
	$i_{L2,T0}$	$\frac{V_C}{L_2} t + I_{1,L2}$	$\frac{V_C + V_{RC}}{L_2} t + I_{1,L2}$
$i_{L,T1}$	$i_{L1,T1}$	$\frac{V_i - V_C}{L_1} t + I_{2,L1}$	$\frac{V_i - (V_C + V_{RC})}{L_1} t + I_{2,L1}$
	$i_{L2,T1}$	$\frac{V_i - V_C}{L_2} t + I_{2,L2}$	$\frac{V_i - (V_C + V_{RC})}{L_2} t + I_{2,L2}$
ΔV_{RC}	-	$\Delta V_C = I_{2,L1} - I_{1,L2} $	
ΔV_{RC}	-	$R_C \Delta C$	

Assuming that $R_{C1} = R_{C2} = R_C$, Table 2 shows the comparison between the values obtained in states with and without presence of ESR capacitors. It is noticeable that other relationships are exactly similar to each other in with and without presence of ESR capacitors.

7. COMPARISON

The proposed buck-boost converter has simple structure. It has two LC networks consists of two inductors and two capacitors. In conventional Z-source, in during the time interval of non-ST state, the diode before the LC network creates an unfavorable operation mode. In addition, diode prevents the reverse current. Thus, using of such converters is limited to such applications which are no need to energy return to input source [1, 25-26]. It should be mentioned that in the proposed converter, the diode before the LC network has not been used.

Without any need to buck and boost transformer or dc/dc converter, the proposed converter can produce lower or higher voltage than the input voltage in its' output. Moreover, due to the existence of LC network, the reliability of converter is increased. This converter

has waveforms with low ripple, so, the additional filter is not needed in circuit.

In conventional Z-H converter, to increase and decrease the output voltage, two separate structures are used (which can be as its' disadvantage) [25, 26]. On the other hand, the conventional dc/dc buck-boost converter is only usable in dc/dc conversion. Whereas, the proposed converter can be used to dc/dc, dc/ac and ac/ac conversion without any change in its' topology. In addition, the gain factor of conventional dc/dc buck-boost converter is equal to $D/(1-D)$. So, the converter will have the maximum voltage gain when duty cycle is close to one. Whereas, the gain factor of the proposed converter is equal to $D/(1-2D)$. Thus, the converter will have the maximum voltage gain when the duty cycle is close to 0.5. Moreover, in comparison with the conventional dc/dc buck-boost converter, the proposed converter has two $D=[0, 0.5)$ and $D=(0.5, 1]$ operating zones. Table 3 shows a comparison between the two structures of conventional Z-H converter in step-down and step-up modes with the proposed Z-H buck-boost converter. Table 4 shows a comparison between conventional Z-source inverter, conventional Z-H buck and boost converters, conventional buck-boost converter and the proposed Z-H buck-boost converter.

8. EXPERIMENTAL RESULTS

The experimental results are used for checking the correct performance of the proposed Z-source converter. The parameters used in experimental are given in Table 5. The experimental results in $D=[0, 0.5)$ operating zone for $B=2$ and $D=0.4$ (boost mode) and for $B=0.5$ and $D=0.25$ (buck mode) are shown in Figs. 6 and 7, respectively.

8.1. Calculation of voltages and currents values

For $B=2$ and $D=0.4$ (boost mode), the following results can be obtained: According to Figs. 4, 5(a) and 6, in operating zone of $D=[0, 0.5)$, from Eq. (9) the value of output voltage is positive and the proposed converter acts as boost in $3^{-1} \leq D \leq 0.5$. From Eqs. (11) and (19), the output voltage and current of converter can be obtained as follows:

$$V_o = BV_i = 2 \times 30 = 60V$$

$$i_o = I_{o,av} = \frac{V_o}{R_L} = \frac{60}{40} = 1.5A$$

In first operating, considering Figs. 4, 5(a) and 6, from Eq. (7) the values of the average voltages of C_1 and C_2 capacitors are positive, and from Eqs. (3) and

(5), the voltages across the L_1 and L_2 inductors are positive for T_0 time interval and those are negative for T_1 time interval. So, we have:

$$V_{C1} = V_{C2} = V_C = \frac{1-D}{1-2D} V_i = \frac{1-0.4}{1-(2 \times 0.4)} \times 30 = 90V$$

$$v_{L1,T0} = v_{L2,T0} = v_{L,T0} = V_C = 90V$$

$$v_{L1,T1} = v_{L2,T1} = v_{L,T1} = V_i - V_C = 30 - 90 = -60V$$

From Eqs. (26) and (27), the current ripple of L_1 inductor and its' average value are equal to:

$$\Delta I_{L1} = \left| \frac{D(1-D)}{1-2D} \right| \frac{V_i}{L_f} = \left| \frac{0.4(1-0.4)}{1-(2 \times 0.4)} \right| \frac{30}{100} = 1.2 \times 0.3 = 0.36A$$

$$I_{L1,av} = (1+B)I_{o,av} = (1+2) \times 1.5 = 4.5A$$

Also, from Eqs. (26) and (28), the current ripple of L_2 inductor and its' average value are given by:

$$\Delta I_{L2} = \left| \frac{D(1-D)}{1-2D} \right| \frac{V_i}{L_f} = \left| \frac{0.4(1-0.4)}{1-(2 \times 0.4)} \right| \frac{30}{100} = 0.36A$$

$$I_{L2,av} = BI_{o,av} = 2 \times 1.5 = 3A$$

From Eqs. (20) and (21), in the first operating zone and during T_0 time interval, the currents through the inductors are increased and from Eqs. (22) and (23), those are decreased in during T_1 time interval (Figs. 5(a) and 6). Hence, from Eqs. (32) to (35), the currents through the L_1 and L_2 inductors at the end of T_0 and T_1 time intervals can be calculated as follows:

$$I_{2,L1} = \frac{2I_{L1,av} + \Delta I_{L1}}{2} = \frac{(2 \times 4.5) + 0.36}{2} = 4.68A$$

$$I_{1,L1} = \frac{2I_{L1,av} - \Delta I_{L1}}{2} = \frac{(2 \times 4.5) - 0.36}{2} = 4.32A$$

$$I_{2,L2} = \frac{2I_{L2,av} + \Delta I_{L2}}{2} = \frac{(2 \times 3) + 0.36}{2} = 3.18A$$

$$I_{1,L2} = \frac{2I_{L2,av} - \Delta I_{L2}}{2} = \frac{(2 \times 3) - 0.36}{2} = 2.82A$$

According to Figs. 5(a) and 6, in the first operating zone and both during T_0 and T_1 time intervals, the currents through the capacitors have falling modes. Hence, from Eqs. (36) and (37), the capacitors current at the end of T_0 and T_1 time intervals are equal to:

$$I'_{2,C1} = I'_{2,C2} = I'_2 = -I_{2,L1} = -4.68A$$

$$I'_{1,C1} = I'_{1,C2} = I'_1 = I_{1,L2} = 2.82A$$

From Eq. (39), the voltage ripple across the capacitors is given by:

$$\Delta V_{C1} = \Delta V_{C2} = \Delta V_C = \left| \frac{D(I_{L1,av})}{Cf} \right| = \left| \frac{0.4 \times 4.5}{470 \times 10^{-3}} \right| = 3.83V$$

Table 3. Comparison between the two structures of conventional Z-H converter in step-down and step-up modes with the proposed Z-H buck-boost converter.

dc/dc Power Conversion	The conventional Z-H buck converter		The conventional Z-H boost converter		The proposed Z-H buck-boost converter	
	T_0 time interval	T_1 time interval	T_0 time interval	T_1 time interval	T_0 time interval	T_1 time interval
V_C	DV_i	DV_i	$\frac{1-D}{1-2D}V_i$	$\frac{1-D}{1-2D}V_i$	$\frac{1-D}{1-2D}V_i$	$\frac{1-D}{1-2D}V_i$
v_L	$(1-D)V_i$	$-DV_i$	$\frac{1-D}{1-2D}V_i$	$-\frac{D}{1-2D}V_i$	$\frac{1-D}{1-2D}V_i$	$-\frac{D}{1-2D}V_i$
V_o	$(1-2D)V_i$	$(1-2D)V_i$	$\frac{1}{1-2D}V_i$	$\frac{1}{1-2D}V_i$	$\frac{D}{1-2D}V_i$	$\frac{D}{1-2D}V_i$
ΔI_L	$D(1-D)\frac{V_i}{L_f}$		$\frac{D(1-D)}{1-2D}\frac{V_i}{L_f}$		$\frac{D(1-D)}{1-2D}\frac{V_i}{L_f}$	

Table 4. Comparison of characteristics for variety of the buck and boost converters.

Converter	Voltage gain (V_o/V_i)	Advantages	Disadvantages	Description
The conventional Z-source converter	$\frac{M}{1-2D}$	<ul style="list-style-type: none"> Having two operating zones Step-down and step-up capability Employing in all of conversions 	<ul style="list-style-type: none"> Needing one switch (or diode) before the LC network Diode prevents the reverse current. 	Diode creates an unpleasant operation mode in during the non-ST switching state.
The conventional Z-H boost converter	$\frac{1}{1-2D}$	<ul style="list-style-type: none"> Having two operating zones Elimination diode before the LC network Employing in all of conversions without any change in its' topology 	Needing four bidirectional switches in all of conversions	It has only step-up capability.
The conventional Z-H buck converter	$1-2D$	<ul style="list-style-type: none"> Having two operating zones Elimination diode before the LC network Employing in all of conversions without any change in its' topology 	<ul style="list-style-type: none"> Needing four unidirectional switches in dc/dc, dc/ac and ac/dc conversions Needing four bidirectional switches in ac/ac conversions 	It has only step-down capability.
The conventional buck-boost converter	$\frac{D}{1-D}$	<ul style="list-style-type: none"> Needing one unidirectional switch Step-down and step-up capability 	<ul style="list-style-type: none"> Only can be used in dc/dc conversion Having one operating zones 	Duty cycle is equal to D in the equation denominator of gain factor of converter. So, the converter will have the maximum voltage gain when duty cycle is close to one.
The proposed Z-H buck-boost converter	$\frac{D}{1-2D}$	<ul style="list-style-type: none"> Having two operating zones Elimination diode before the LC network Step-down and step-up capability Employing in dc/dc, dc/ac and ac/ac conversions without any change in its' topology 	Needing four bidirectional switches	In the proposed converter, the value of duty cycle has been changed from D to $2D$ in the equation denominator of gain factor of converter. So, the converter will have the maximum voltage gain when duty cycle is close to half.

Table 5. The parameters of converter.

Input voltage (V_i)	Impedance-source network		Load (R_L)	Switching frequency (f)
	$C_1 = C_2$	$L_1 = L_2$		
30V	$47\mu F$	$10mH$	40Ω	$10kHz$

From Eqs. (40) and (41), in the first operating zone, the current through input source has constant value in during T_0 time interval, and it is decreased in during T_1 time interval (Figs. 5(a) and 6), so, we have:

$$I_2'' = -i_o = -1.5A$$

$$I_1'' = 2I_{1,L2} = 2 \times 2.82 = 5.64A$$

From Eq. (25), the average current of input voltage source can be obtained as follows:

$$I_{i,av} = BI_{o,av} = 2 \times 1.5 = 3A$$

8.1. Design the values of inductors and capacitors
 For $D = 0.4$, $\Delta I_{L1} = \Delta I_{L2} = 0.36$ and $\Delta V_{C1} = \Delta V_{C2} = 3.83$, the values of inductors and capacitors can be calculated as follows:

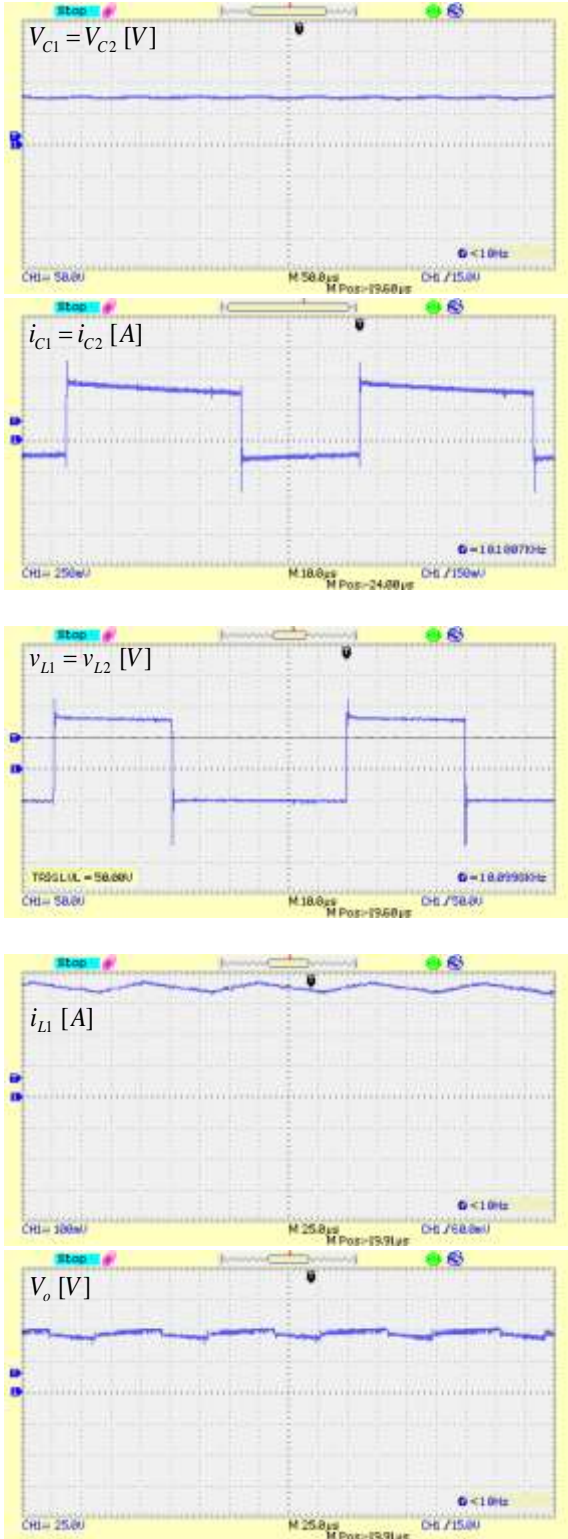


Fig. 6. Experimental results in $D=[0, 0.5]$ operating zone for $B=2$ and $D=0.4$ (boost mode).

From Eq. (42), the allowable voltage ripple $x_c\%$ is given by:

$$x_{C1}\% = x_{C2}\% = x_c\% = \frac{\Delta V_C}{V_C} = \frac{3.83}{90} = 0.042$$

From Eq. (43), the rated value of C_1 and C_2 capacitances is equal to:

$$C_1 = C_2 = \frac{D^2}{f R_L (1-2D)x_c\%} = \frac{(0.4)^2}{(80 \times 10^3)(0.042)} \approx 47 \mu F$$

From Eqs. (44) and (45), the allowable current ripples $x_{L1}\%$ and $x_{L2}\%$ are given by:

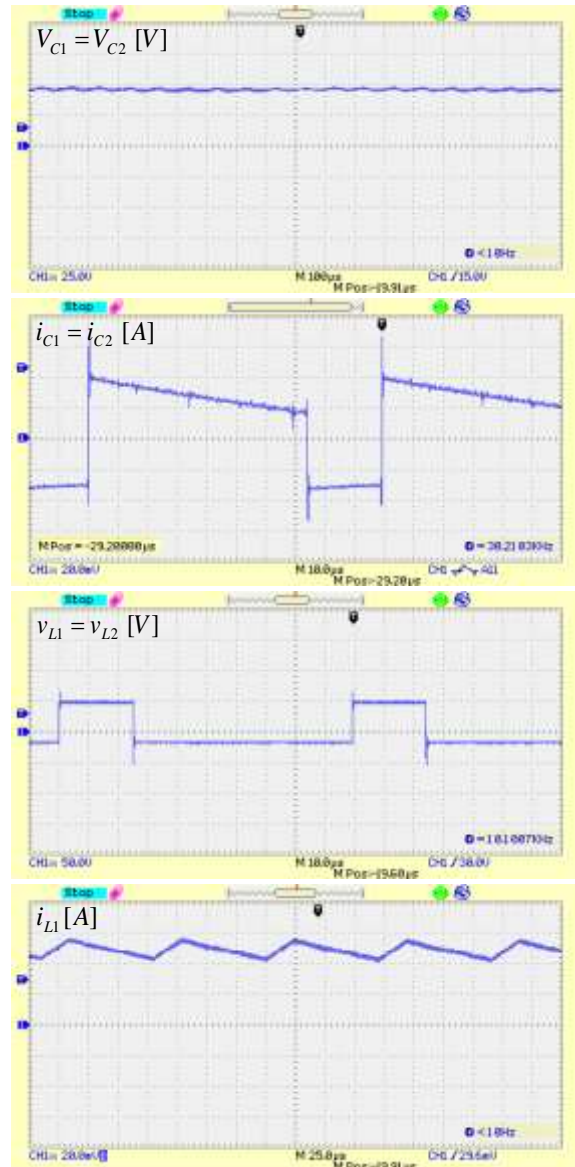
$$x_{L1}\% = \frac{\Delta I_{L1}}{I_{L1,av}} = \frac{0.36}{4.5} = 0.08$$

$$x_{L2}\% = \frac{\Delta I_{L2}}{I_{L2,av}} = \frac{0.36}{3} = 0.12$$

From Eqs. (46) and (47), the rated values of L_1 and L_2 inductances are equal to:

$$L_1 = \frac{R_L(1-2D)}{f x_{L1}\%} = \frac{40(1-0.8)}{(10 \times 10^3)(0.08)} = 10mH$$

$$L_2 = \frac{R_L(1-D)(1-2D)}{Df x_{L2}\%} = \frac{40(0.6)(0.2)}{(4000)(0.12)} = 10mH$$



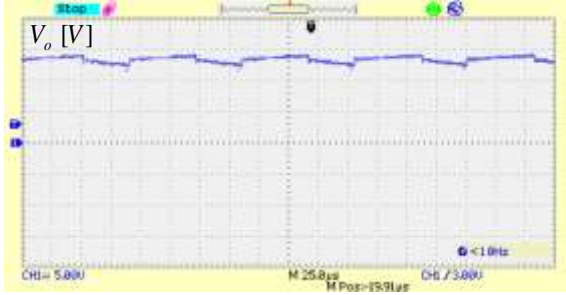


Fig. 7. Experimental results in $D=[0, 0.5)$ operating zone for $B=0.5$ and $D=0.25$ (buck mode).

Considering theoretical values calculated for the boost operation in $D=[0, 0.5)$ operating zone, it is observed that the given experimental results in Fig. 6 are similar to both theoretical results and Fig. 5(a).

For $B=0.5$ and $D=0.25$ (buck mode), the following results can be obtained:

According to Figs. 4, 5(a) and 7, in operating zone of $D=[0, 0.5)$, from (9) the value of output voltage is positive and the proposed converter acts as buck in $0 \leq D \leq \frac{1}{3}$. So, from Eqs. (11) and (19), the output voltage and current of converter can be obtained as follows:

$$V_o = BV_i = 0.5 \times 30 = 15V$$

$$i_o = I_{o,av} = \frac{V_o}{R_L} = \frac{15}{40} = 0.375A$$

In first operating, considering Figs. 4, 5(a) and 7, from Eq. (7) the values of the average voltages of C_1 and C_2 capacitors are positive, and from Eqs. (3) and (5), the voltages across the L_1 and L_2 inductors are positive for T_0 time interval and those are negative for T_1 time interval. So, we have:

$$V_{C1} = V_{C2} = V_C = \frac{1-D}{1-2D} V_i = \frac{1-0.25}{1-(2 \times 0.25)} \times 30 = 45V$$

$$v_{L1,T0} = v_{L2,T0} = v_{L,T0} = V_C = 45V$$

$$v_{L1,T1} = v_{L2,T1} = v_{L,T1} = V_i - V_C = 30 - 45 = -15V$$

From Eqs. (26) and (27), the current ripple of L_1 inductor and its' average value are equal to:

$$\Delta I_{L1} = \left| \frac{D(1-D)}{1-2D} \right| \frac{V_i}{L_f} = \left| \frac{0.25(1-0.25)}{1-(2 \times 0.25)} \right| \frac{30}{100} = 0.375 \times 0.3 = 0.11A$$

$$I_{L1,av} = (1+B)I_{o,av} = (1+0.5) \times 0.375 = 0.56A$$

Also, from Eqs. (26) and (28), the current ripple of L_2 inductor and its' average value are given by:

$$\Delta I_{L2} = \left| \frac{D(1-D)}{1-2D} \right| \frac{V_i}{L_f} = \left| \frac{0.25(1-0.25)}{1-(2 \times 0.25)} \right| \frac{30}{100} = 0.11A$$

$$I_{L2,av} = BI_{o,av} = 0.5 \times 0.375 = 0.19A$$

From Eqs. (20) and (21), in the first operating zone and during T_0 time interval, the currents through the inductors are increased and from Eqs. (22) and (23), those are decreased in during T_1 time interval (Figs. 5(a) and 7). Hence, from Eqs. (32) to (35), the currents through the L_1 and L_2 inductors at the end of T_0 and T_1 time intervals can be calculated as follows:

$$I_{2,L1} = \frac{2I_{L1,av} + \Delta I_{L1}}{2} = \frac{(2 \times 0.56) + 0.11}{2} = 0.61A$$

$$I_{1,L1} = \frac{2I_{L1,av} - \Delta I_{L1}}{2} = \frac{(2 \times 0.56) - 0.11}{2} = 0.5A$$

$$I_{2,L2} = \frac{2I_{L2,av} + \Delta I_{L2}}{2} = \frac{(2 \times 0.19) + 0.11}{2} = 0.24A$$

$$I_{1,L2} = \frac{2I_{L2,av} - \Delta I_{L2}}{2} = \frac{(2 \times 0.19) - 0.11}{2} = 0.13A$$

According to Figs. 5(a) and 7, in the first operating zone and both during T_0 and T_1 time intervals, the currents through the capacitors have falling modes. Hence, from Eqs. (36) and (37), the capacitors current at the end of T_0 and T_1 time intervals are equal to:

$$I'_{2,C1} = I'_{2,C2} = I'_2 = -I_{2,L1} = -0.61A$$

$$I'_{1,C1} = I'_{1,C2} = I'_1 = I_{1,L2} = 0.13A$$

From Eqs. (39), the voltage ripple across the capacitors is given by:

$$\Delta V_{C1} = \Delta V_{C2} = \Delta V_C = \left| \frac{D(I_{L1,av})}{C_f} \right| = \left| \frac{0.25 \times 0.56}{470 \times 10^{-3}} \right| = 0.3V$$

From Eqs. (40) and (41), in the first operating zone, the current through input source has constant value in during T_0 time interval, and it is decreased in during T_1 time interval (Figs. 5(a) and 7), so, we have:

$$I_2'' = -i_o = -0.375A$$

$$I_1'' = 2I_{1,L2} = 2 \times 0.13 = 0.26A$$

From Eqs. (25), the average current of input voltage source can be obtained as follows:

$$I_{i,av} = BI_{o,av} = 0.5 \times 0.375 = 0.19A$$

Considering theoretical values calculated for the buck operation in $D=[0, 0.5)$ operating zone, it is observed that the given experimental results in Fig. 7 are similar to both theoretical results and Fig. 5(a).

9. CONCLUSIONS

In this paper, a new Z-source buck-boost converter based on Z-H was proposed. The main advantages of the proposed converter are simple topology, employing in dc/dc, dc/ac and ac/ac conversion, step-up and step-down capabilities, and low ripple. In this paper, the operating principle of the proposed converter in dc/dc conversion with details and complete equations were explained. Moreover, the calculations of inductors and capacitors ripples, the power losses and efficiency and optimum values of inductors and capacitors have been presented. The experimental results reconfirm the correctness of analysis and good performance of the proposed converter.

REFERENCES

- [1] F.Z. Peng, "Z-source inverter," *IEEE Trans. Ind. Appl.*, vol. 39, no. 2, pp. 504-510, 2003.
- [2] S. Torabzad, E. Babaei, and M. Kalantari, "Z-source inverter based dynamic voltage restorer," in *Proce. of the PEDSTC*, pp. 406-411, 2010.
- [3] X. Ding, Z. Qian, Y. Xie, and F.Z. Peng, "Transient modeling and control of the novel ZVS Z-source rectifier," in *Proce. of the PESC*, pp. 1-5, 2006.
- [4] M.R. Banaei, R. Alizadeh, N. Jahanyari, and E. Seifi Najmi, "An ac Z-source converter based on gamma structure with safe-commutation strategy," *IEEE Trans. Power Electron.*, vol. 31, no. 2, pp. 1255-1262, 2016.
- [5] F. Sedaghati, and E. Babaei, "Double input dc-dc Z-source converter," in *Proce. of the PEDSTC*, pp. 581-586, 2011.
- [6] F.Z. Peng, M. Shen, and Z. Qian, "Maximum boost control of the Z-source inverter," *IEEE Trans. Power Electron.*, vol. 20, no. 4, pp. 833-838, 2005.
- [7] M. Shen, J. Wang, A. Joseph, F.Z. Peng, L.M. Tolbert, and D.J Adams, "Constant boost control of the Z-source inverter to minimize current ripple and voltage stress," *IEEE Trans. Ind. Appl.*, vol. 42, no. 3, pp. 770-778, 2006.
- [8] S.R. Aghdam, E. Babaei, and S. Laali, "Maximum constant boost control method for switched-inductor Z-source inverter by using battery," in *Proc. of the IECON*, 2013, pp. 984-989.
- [9] N. Mirkazemian and E. Babaei, "A new topology for quasi-Z-source inverter," in *Proce. of the PSC*, 2015, pp. 1-7.
- [10] H. Rostami, and D.A. Khaburi, "Voltage gain comparison of different control methods of the Z-source inverter," in *Proc. of the ELECO*, pp. 268-272, 2009.
- [11] U.S. Ali, and V. Kamaraj, "A novel space vector PWM for Z-source inverter," in *Proc. of the ICEES*, pp. 82-85, 2011.
- [12] J.W. Jung, and A. Keyhani, "Control of a fuel cell based Z-source converter," *IEEE Trans. Energy Convers.*, vol. 22, no. 2, pp. 467-476, 2007.
- [13] O. Ellabban, J.V. Mierlo, and P. Lataire, "Experimental study of the shoot-through boost control methods for the Z-source inverter," *EPEJ*, vol. 21, no. 2, pp. 18-29, 2011.
- [14] Y. Liu, B. Ge, F.J.T.E. Ferreira, A.T. de Almeida, and H.A. Rub, "Modelling and SVPWM control of quasi-Z-source inverter," in *Proc. of the EPQU*, pp. 1-7, 2011.
- [15] Y. Liu, B. Ge, H.A. Rub, and F.Z. Peng, "Overview of space vector modulations for three-phase Z-source/quasi-Z-source inverters," *IEEE Trans. Power Electron.*, vol. 29, no. 4, pp. 2098-2108, 2014.
- [16] Y. Liu, B. Ge, and H.A. Rub, "Theoretical and experimental evaluation of four space vector modulations applied to quasi-Z-source inverters," *IET Power Electron.*, vol. 6, no. 7, pp. 1257-1269, 2013.
- [17] Y.P. Siwakoti, and G.E. Town, "Three-phase transformerless grid connected quasi Z-source inverter for solar photovoltaic systems with minimal leakage current," in *Proc. of the PEDG*, pp. 368-373, 2012.
- [18] F. Bradaschia, M.C. Cavalcanti, P.E.P. Ferraz, F.A.S. Neves, E.C. dos Santos, and J.H.G.M. da Silva, "Modulation for three-phase transformer-less Z-source inverter to reduce leakage currents in photovoltaic systems," *IEEE Trans. Ind. Electron.*, vol. 58, no. 12, pp. 5385-5395, 2011.
- [19] Y.P. Siwakoti, and G.E. Town, "Common-mode voltage reduction techniques of three-phase quasi Z-source inverter for AC drives," in *Proc. of the APEC*, 2013, pp. 2247-2252.
- [20] S.R. Aghdam, E. Babaei, and S. Ghasemzadeh, "Improvement the performance of switched-inductor Z-source inverter," in *Proc. of the IECON*, 2013, pp. 876-881.
- [21] M.S. Zarbil, E. Shokati Asl, E. Babaei, and M. Sabahi, "A new structure for quasi-Z-source inverter based on switched inductors and transformer," *Iran. Electr. Ind. J. Qual. Prod.*, vol. 4, no. 8, pp. 63-73, 2016.
- [22] E. Babaei, M. Hasan Babayi, E. Shokati Asl, and S. Laali, "A new topology for Z-source inverter based on switched-inductor and boost Z-source inverter," *J. Oper. Autom. Power Eng.*, vol. 3, no. 2, pp. 167-184, 2015.
- [23] E. Babaei, E. Shokati Asl, M.H. Babayi, "Steady-state and small-signal analysis of high voltage gain half-bridge switched-boost inverter," *IEEE Trans. Ind. Electron.*, vol. 63, no. 6, pp. 3546-3553, 2016.
- [24] R. Strzelecki, and N. Strzelecka, "Simulation investigation of the Z-source NPC inverter," *Doctoral school of energy- and geo-technology, Kuressaare, Estonia*, pp. 213-218, 2007.
- [25] F. Zhang, F.Z. Peng, and Z. Qian, "Z-H converter," in *Proce. of the PESC*, 2008, pp. 1004-1007.
- [26] T. Ahmadzadeh, and E. Babaei, "Z-H buck converter: Analysis and simulation," in *Proc. of the PEDSTC*, pp. 436-441, 2015.
- [27] E. Babaei, M. Hasan Babayi, E. Shokati Asl, S. Laali, "A new topology for Z-source inverter based on switched-inductor and boost Z-source inverter," *J. Oper. Autom. Power Eng.*, vol. 2, no. 2, pp. 167-184, 2015.
- [28] V.P. Galigekere and M.K. Kazimierczuk, "Analysis of PWM Z-source dc-dc converter in CCM for steady-state," *IEEE Trans. Circuits Syst. I Reg. Papers*, vol. 59, no. 4, pp. 854-863, 2012.
- [29] E. Babaei, E. Shokati Asl, M.H. Babayi, and S. Laali, "Developed embedded switched-Z-source inverter," *IET Power Electron.*, vol. 9, no. 9, pp. 1828-1841, 2016.